eLIFE elifesciences.org

RESEARCH ARTICLE

Figures and figure supplements

The postsynaptic t-SNARE Syntaxin 4 controls traffic of Neuroligin 1 and Synaptotagmin 4 to regulate retrograde signaling

Kathryn P Harris *et al*

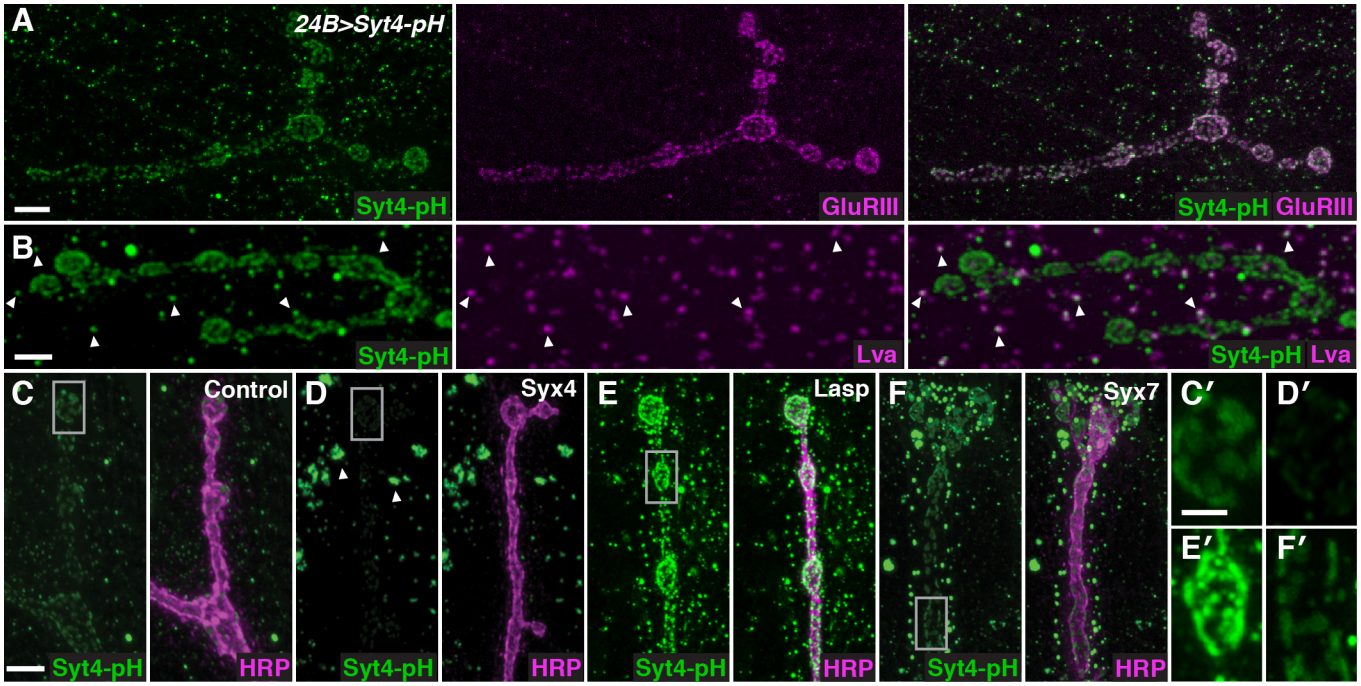

Figure 1. A candidate RNAi screen for regulators of postsynaptic exocytosis. (**A,B**) Representative images of Syt4-pH expressed with the postsynaptic muscle driver 24B-GAL4. Syt4-pH (green) accumulates in postsynaptic membrane that also contains domains of GluRIII (magenta) (**A**). Syt4-pH also decorates numerous cytoplasmic puncta, many of which overlap with the Golgi marker Lva (magenta), arrowheads (**B**). (**C–F**) Examples of candidate RNAis affecting Syt4-pH localization: control (**C**); *Syx4-RNAi* reduces Syt4-pH at the membrane and causes a redistribution to prominent cytoplasmic puncta, arrowheads (**D**); *Lasp-RNAi* increases Syt4-pH at the membrane (**E**); and *Syx7-RNAi* causes a redistribution of Syt4-pH puncta around the NMJ without affecting the intensity at the membrane (**F**). (**C′–F′**) Close-ups of **C–F**. Scale bars = 7 μm (**A**), 5 μm (**B–F**), 2 μm (**C′–F′**).
DOI: 10.7554/eLife.13881.003

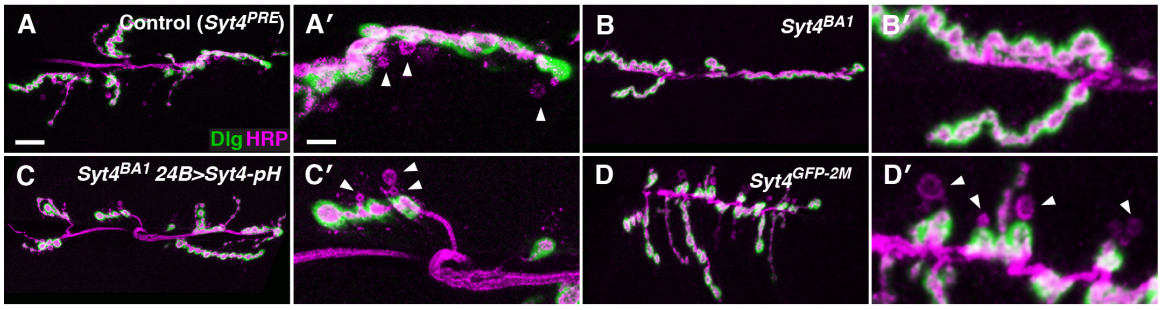

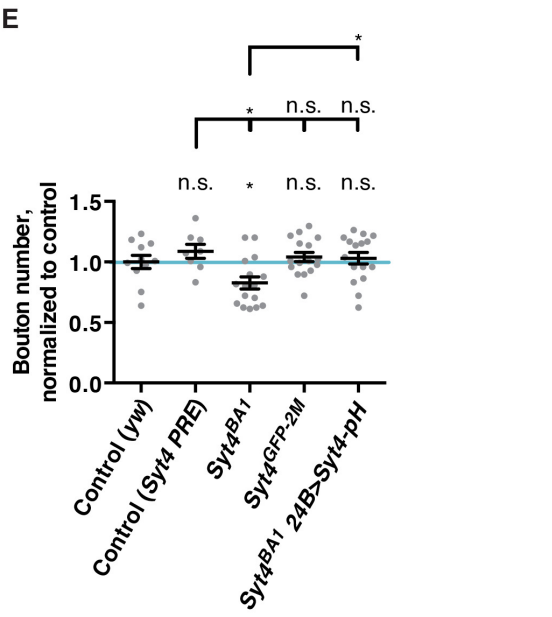

	n	mean	SEM
Control (*Syt4*^{PRE})	8	1.088	0.0574
Control (*yw*)	11	1.001	0.0542
Syt4^{BA1}	16	0.827	0.0494
Syt4^{GFP-2M}	16	1.041	0.0387
Syt4^{BA1} *24B>Syt4-pH*	16	1.031	0.0486

Comparison	Adjusted P Value (ANOVA)
Control (*Syt4*^{PRE}) vs. Control (*yw*)	0.835
Control (*Syt4*^{PRE}) vs. *Syt4*^{BA1}	0.0118
Control (*Syt4*^{PRE}) vs. *Syt4*$^{GFP-2M}$	0.9743
Control (*Syt4*^{PRE}) vs. *Syt4*^{BA1} *24B>Syt4-pH*	0.9487
Control (*yw*) vs. *Syt4*^{BA1}	0.0425
Control (*yw*) vs. *Syt4*$^{GFP-2M}$	0.9789
Control (*yw*) vs. *Syt4*^{BA1} *24B>Syt4-pH*	0.9928
Syt4^{BA1} vs. *Syt4*^{BA1} *24B>Syt4-pH*	0.0176

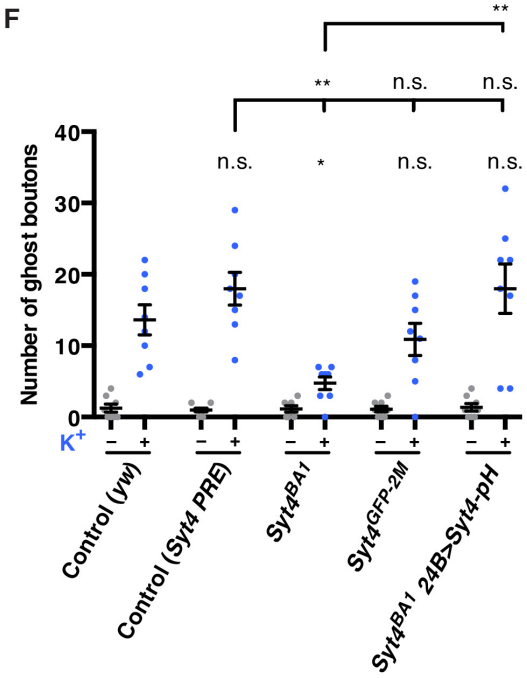

	n	mean	SEM
Control (*Syt4*^{PRE}) baseline	8	1	0.2673
Control (*Syt4*^{PRE}) high K$^+$	8	18	2.299
Control (*yw*) baseline	8	1.25	0.559
Control (*yw*) high K$^+$	8	13.63	2.104
Syt4^{BA1} baseline	7	1.143	0.4592
Syt4^{BA1} high K$^+$	8	4.75	0.8814
Syt4^{GFP-2M} baseline	8	1.125	0.3981
Syt4^{GFP-2M} high K$^+$	8	10.88	2.248
Syt4^{BA1} *24B>Syt4-pH* baseline	8	1.375	0.5324
Syt4^{BA1} *24B>Syt4-pH* K$^+$	8	18	3.459

Comparison	Adjusted P value (ANOVA)
Control (*yw*) high K$^+$ vs. Control (*Syt4*^{PRE}) high K$^+$	0.6815
Control (*yw*) high K$^+$ vs. *Syt4*^{BA1} high K$^+$	0.0483
Control (*yw*) high K$^+$ vs. *Syt4*$^{GFP-2M}$ high K$^+$	0.9198
Control (*yw*) high K$^+$ vs. *Syt4*^{BA1} *24B>Syt4-pH* high K$^+$	0.6815
Control (*Syt4*^{PRE}) high K$^+$ vs. *Syt4*^{BA1} high K$^+$	0.0028
Control (*Syt4*^{PRE}) high K$^+$ vs. *Syt4*$^{GFP-2M}$ high K$^+$	0.2233
Control (*Syt4*^{PRE}) high K$^+$ vs. *Syt4*^{BA1} *24B>Syt4-pH* high K$^+$	> 0.9999
Syt4^{BA1} high K$^+$ vs. *Syt4*^{BA1} *24B>Syt4-pH* high K$^+$	0.0028

Figure 1—figure supplement 1. Both Syt4-GFP CRISPR knock-in and overexpression of Syt4-pH can replace endogenous Syt4 with respect to synaptic architecture and plasticity. (**A–D**) Representative images of NMJs stained with antibodies to HRP (magenta) and the postsynaptic marker Dlg (green) to

Figure 1—figure supplement 1 continued on next page

Figure 1—figure supplement 1 continued

highlight synaptic boutons. Acute budding of new varicosities ("ghost boutons") was stimulated with spaced incubations in high K^+. Ghost boutons are identified as round HRP+ structures lacking Dlg signal (arrowheads). Images are shown from the control genotype $Syt4^{PRE}$ (**A,A'**), a precise excision line that serves as a genetic background control for the $Syt4^{BA1}$ allele (**B,B'**). Also shown are images from animals expressing *Syt4-pH* postsynaptically in the *Syt4* null background ($Syt4^{BA1}$ *24B>Syt4-pH*; **C,C'**), and the CRISPR GFP knock-in line $Syt4^{GFP\text{-}2M}$ (**D,D'**). (**E**) Quantification of bouton number normalized to *yw*, a genetic background control for $Syt4^{GFP\text{-}2M}$. Blue line indicates the *yw* control mean. Data are presented as mean ± SEM. (**F**) Quantification of ghost bouton number per NMJ from animals without (–) or with (+) high K^+ stimulation. Data are presented as mean ± SEM. $Syt4^{BA1}$ *24B>Syt4-pH* animals have a normal number of boutons and exhibit normal budding of ghost boutons compared to the $Syt4^{PRE}$ control, and are significantly rescued compared to $Syt4^{BA1}$. $Syt4^{GFP\text{-}2M}$ animals have a normal number of boutons and exhibit normal budding of ghost boutons compared to the *yw* control line. Scale bars = 20 μm (**A–D**), 6.7 μm (**A'–D'**). Sample size (n), mean, SEM, and pairwise statistical comparisons are presented for the data in (**E**) and (**F**).

DOI: 10.7554/eLife.13881.004

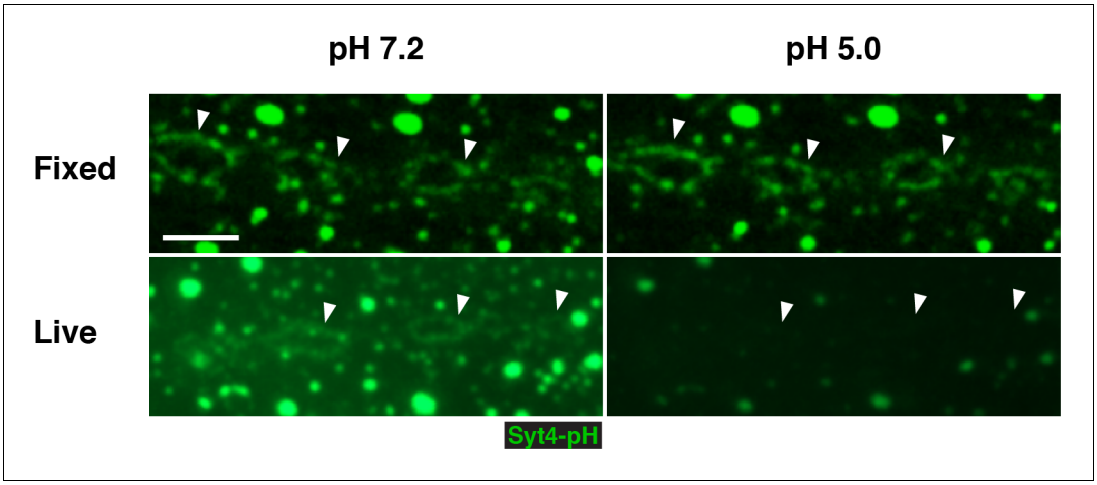

Figure 1—figure supplement 2. pHluorin is quenched in live but not fixed preparations. Animals expressing Syt4-pH in the postsynaptic cell (*24B>Syt4-pH*) were dissected and imaged live or following fixation in paraformaldehyde. The same animal was imaged first following incubation in pH 7.2 HL3.1 buffer and second following incubation in pH 5.0 HL3.1 buffer. Arrows indicate plasma membrane accumulations of Syt4-pH. Scale bars = 2.5 µm.

DOI: 10.7554/eLife.13881.005

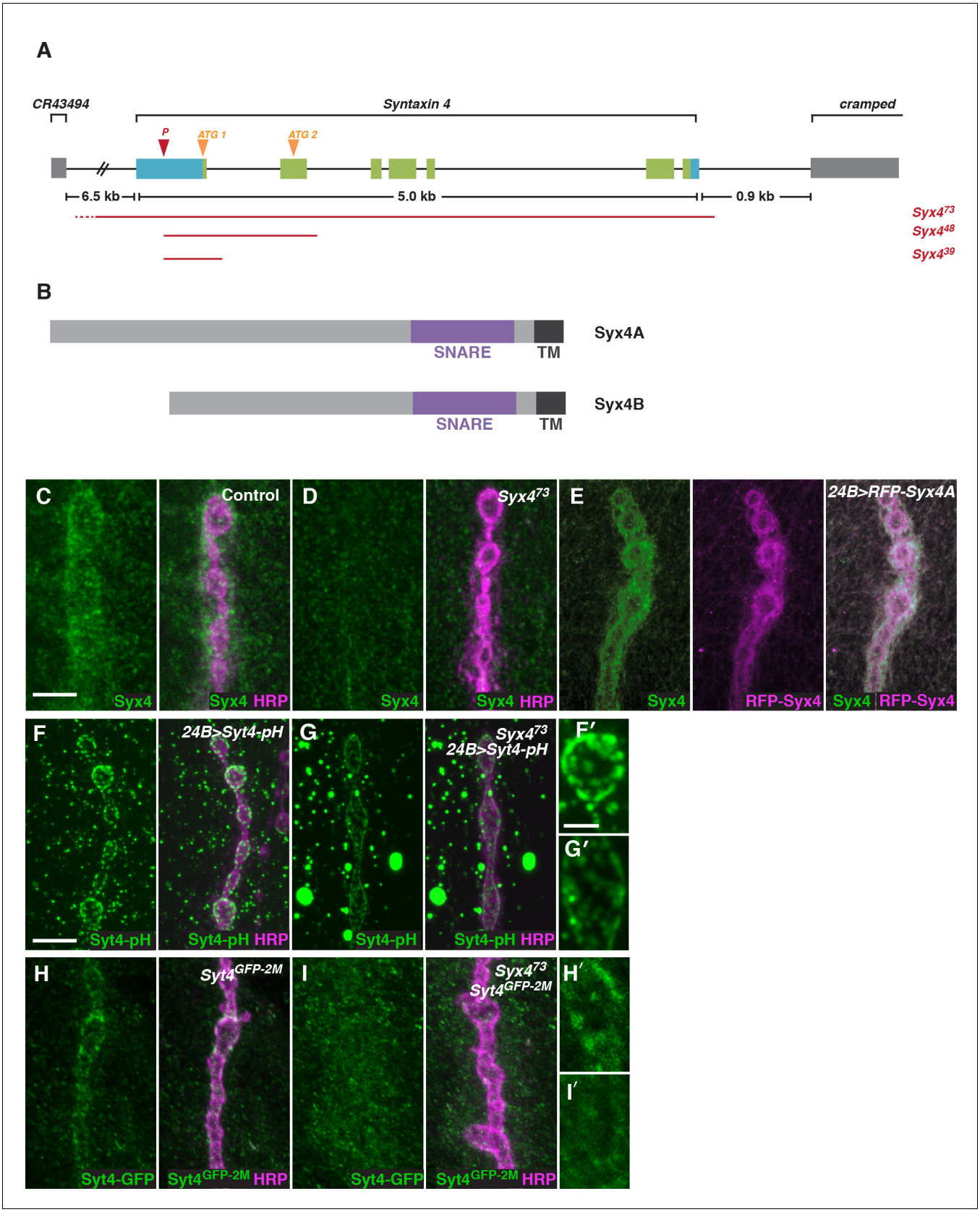

Figure 2. Syntaxin 4 is a postsynaptic plasma membrane SNARE. (**A**) *Syx4* genomic region. Coding exons are indicated in green while non-coding exons are in blue. Two predicted start sites (ATG) are indicated in orange. The location of the P-element used for mutagenesis (P) is indicated in red.

Figure 2 continued on next page

Figure 2 continued

Three alleles of *Syx4* were isolated. Deleted regions are indicated in red. Solid lines indicate regions known to be deleted from PCR analysis and sequencing, while dotted lines indicate regions within which breakpoints have been mapped. (**B**) *Syx4* encodes a protein with an N-terminal domain, a SNARE domain and a C-terminal transmembrane domain. There are two predicted isoforms that differ in the size of the N-terminal domain. (**C,D**) Representative images of NMJs stained for Syx4 (green) and the neuronal membrane marker HRP (magenta). Syx4 staining at the synapse in precise excision control animals (**C**) is absent in $Syx4^{73}$ mutant animals (**D**). (**E**) Representative image from an animal stained for Syx4 (green) and expressing *RFP-Syx4* (magenta) with *24B-GAL4*. (**F,G**) Representative images from animals expressing *Syt4-pH* with *24B-GAL4* in a control (**F**) or $Syx4^{73}$ (**G**) background. Syt4-pH is reduced at the postsynaptic membrane and redistributed to large cytoplasmic accumulations in $Syx4^{73}$ mutants. (**F′,G′**) Close-ups of F and G. (**H,I**) Representative images from $Syt4^{GFP\text{-}2M}$ knock-in animals in a control (H) or $Syx4^{73}$ (I) background. Synaptic localization of $Syt4^{GFP\text{-}2M}$ is reduced in $Syx4^{73}$ mutants. (**H′,I′**) Close-ups of H and I. Scale bars = 5 μm (**C–I**), 2 μm (**F′,G′,H′,I′**).

DOI: 10.7554/eLife.13881.007

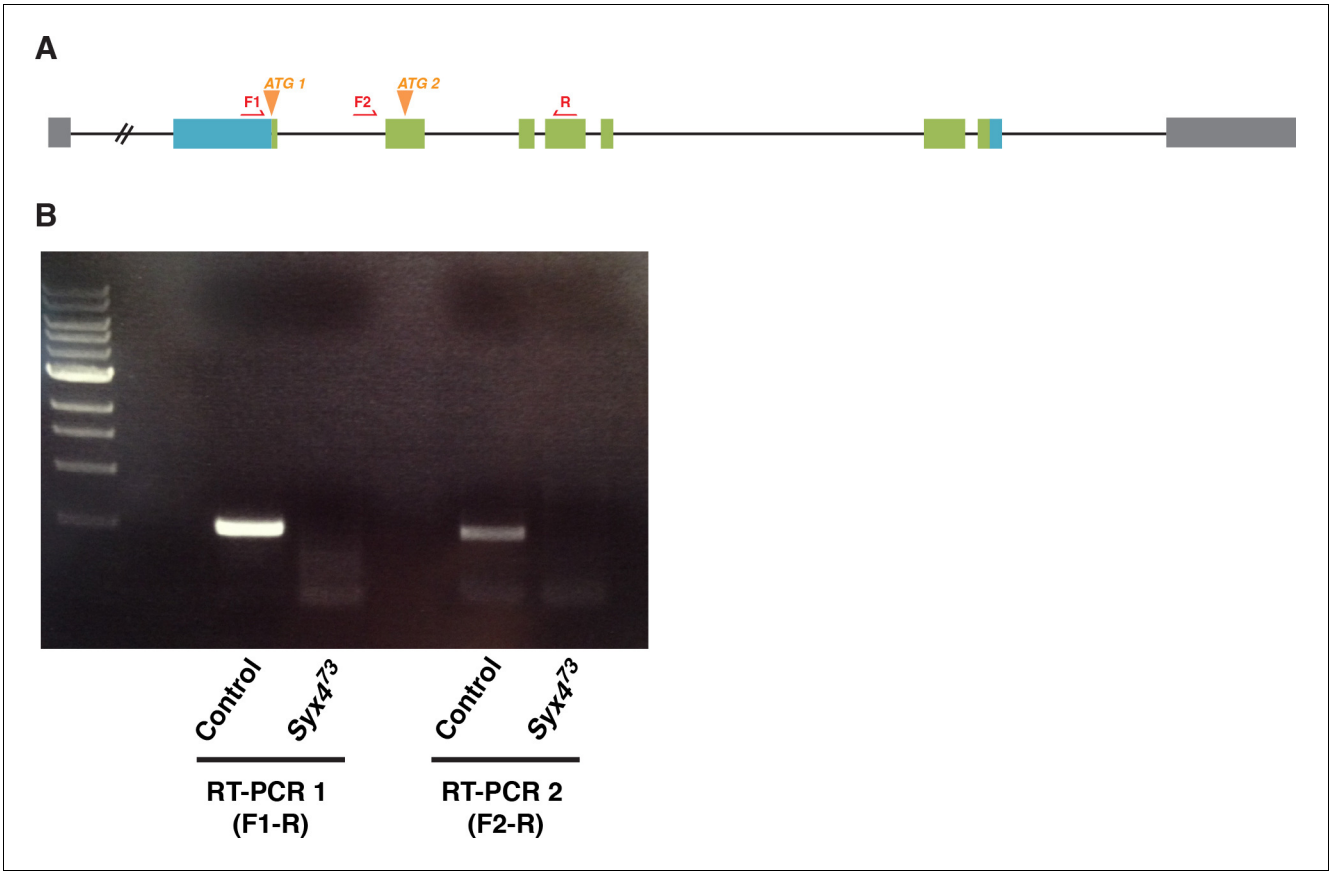

Figure 2—figure supplement 1. RT-PCR analysis of Syntaxin 4. Primers (red arrows) were designed to distinguish *Syx4A* and *Syx4B* transcripts by RT-PCR. F1 and R amplify a product from *Syx4A* transcript and F2 and R amplify a product from *Syx4B* transcript. Both transcripts are detected in control animals and both are absent from $Syx4^{73}$ nulls.

DOI: 10.7554/eLife.13881.008

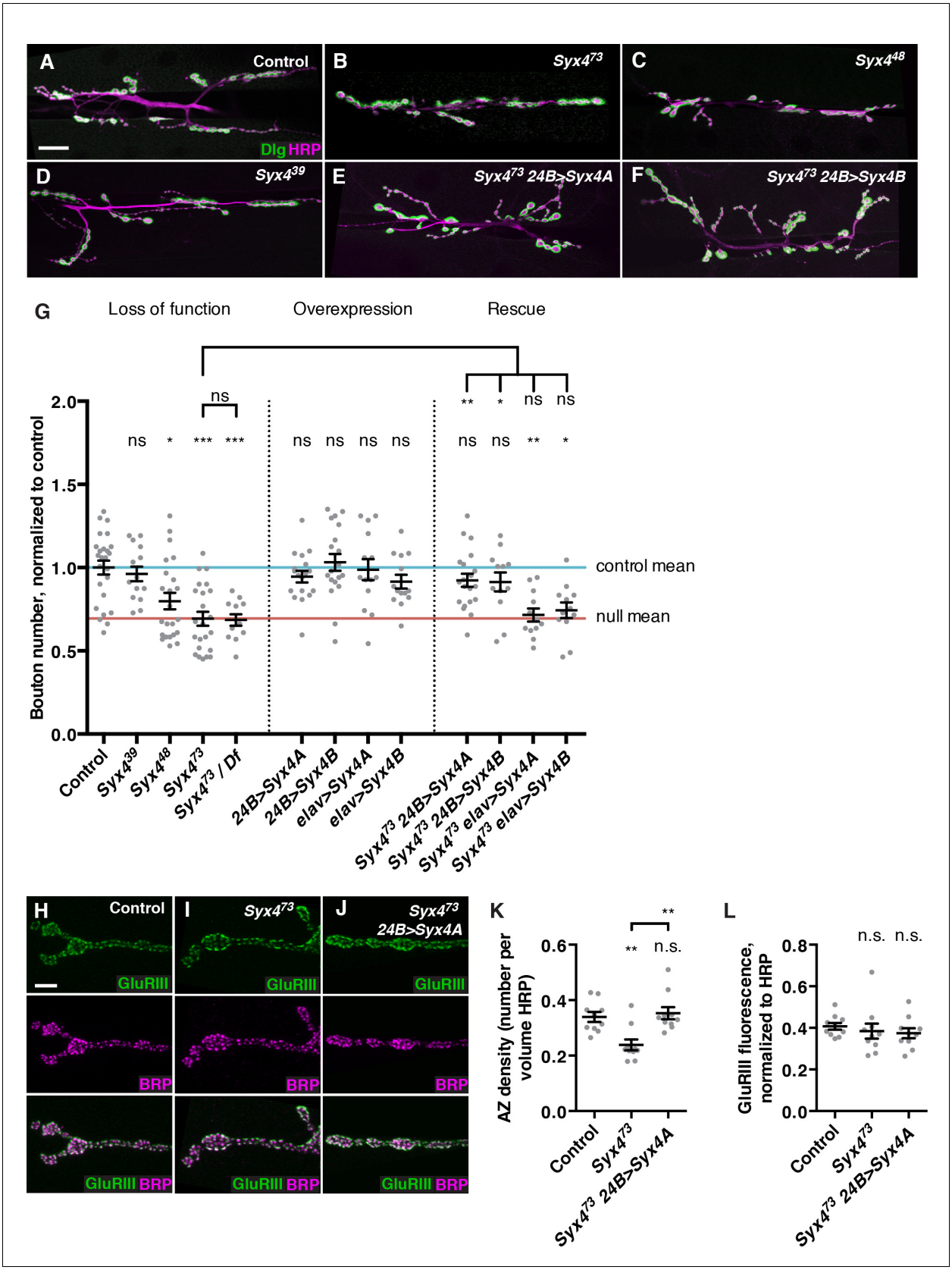

Figure 3. Syntaxin 4 regulates synaptic growth at the NMJ. (**A–F**) Representative images of NMJs stained with antibodies to the postsynaptic marker Dlg (green) and the neuronal membrane marker HRP (magenta) to highlight the number of synaptic boutons; images are shown from precise excision

Figure 3 continued on next page

Figure 3 continued

control (**A**), *Syx4*^{73} (**B**), *Syx4*^{48} (**C**), *Syx4*^{39} (**D**), *Syx4*^{73} *24B>Syx4A* (**E**), and *Syx4*^{73} *24B>Syx4B* (**F**) animals. (**G**) Quantification of bouton number, normalized to controls. Blue line indicates the control mean. Red line indicates *Syx4*^{73} null mean. Data are presented as mean ± SEM. (**H–J**), Representative images of NMJs stained with antibodies to GluRIII (green) and the AZ marker Brp (magenta); images are shown from precise excision control (**H**), *Syx4*^{73} (**I**), and *Syx4*^{73} *24B>Syx4A* (**J**) animals. (**K**), Quantification of AZ density, calculated as the number of AZs per volume HRP. Data are presented as mean ± SEM. (**L**) Quantification of GluRIII fluorescence per HRP fluorescence. Data are presented as mean ± SEM. Scale bars = 20 μm (**A–F**), 5 μm (**H–J**). Statistical comparisons are fully described in Figure 3—source data 1, and are indicated here as ***p<0.001, **p<0.01, *p<0.05, ns = not significant; comparisons are with control unless indicated.

DOI: 10.7554/eLife.13881.009

The following source data is available for figure 3:

Source data 1. Statistical data for ***Figure 3***.

DOI: 10.7554/eLife.13881.010

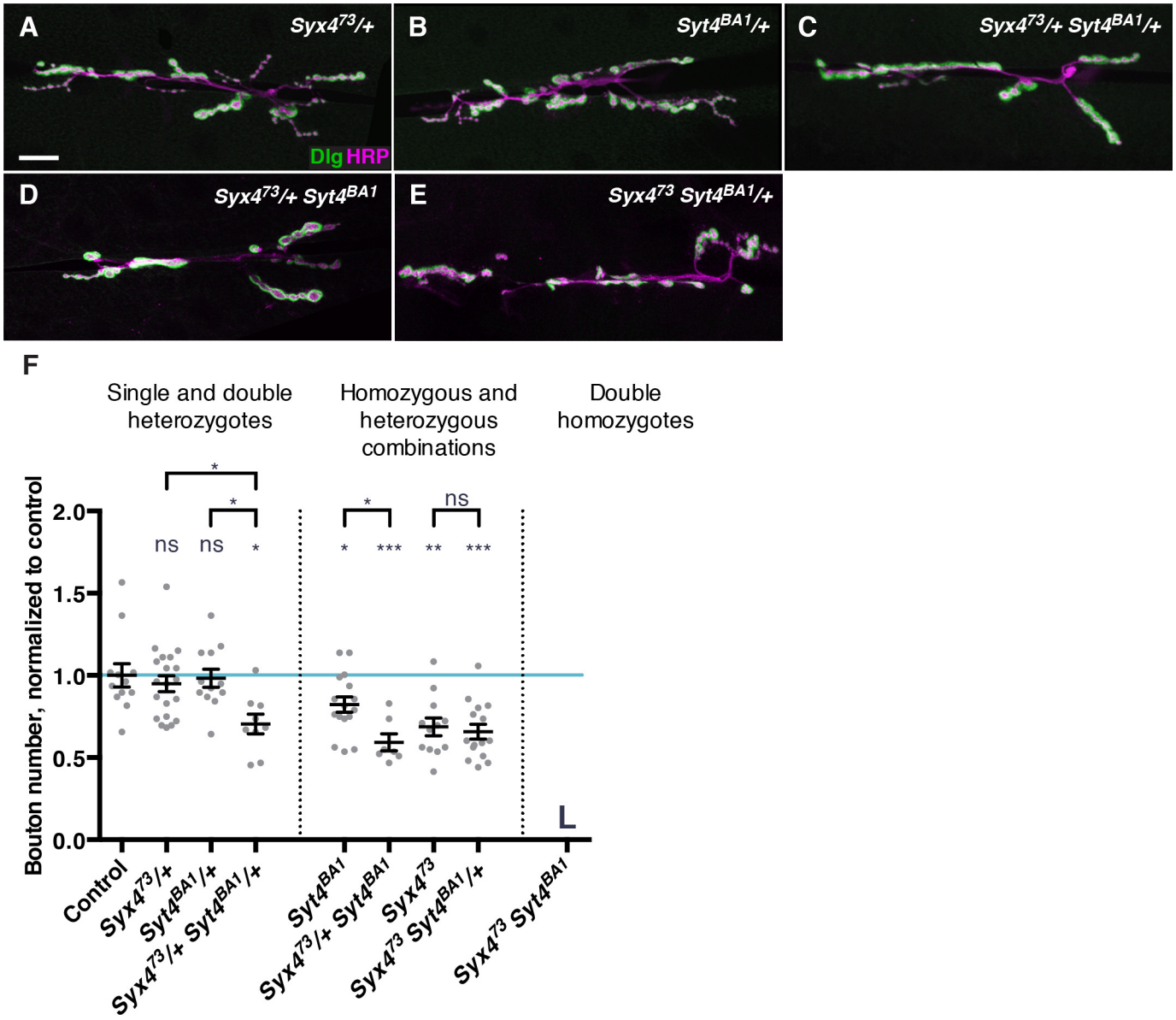

Figure 4. Genetic interactions between Syntaxin 4 and Synaptotagmin 4. (**A–E**) Representative images of NMJs stained with antibodies to the postsynaptic marker Dlg (green) and the neuronal membrane marker HRP (magenta) to highlight the number of synaptic boutons; images are shown from $Syx4^{73}$/+ (**A**), $Syt4^{BA1}$/+ (**B**), $Syx4^{73}$/+ $Syt4^{BA1}$/+ (**C**), $Syx4^{73}$/+ $Syt4^{BA1}$ (**D**), and $Syx4^{73}$ $Syt4^{BA1}$/+ (**E**) animals. (**F**) Quantification of bouton number, normalized to controls. Blue line indicates the control mean. Data are presented as mean ± SEM. L = lethal. Scale bars = 20 μm (**A–E**). Statistical comparisons are fully described in ***Figure 4—source data 1***, and are indicated here as ***p<0.001, **p<0.01, *p<0.05, ns = not significant; comparisons are with control unless indicated.

DOI: 10.7554/eLife.13881.011

The following source data is available for figure 4:

Source data 1. Statistical data for ***Figure 4***.

DOI: 10.7554/eLife.13881.012

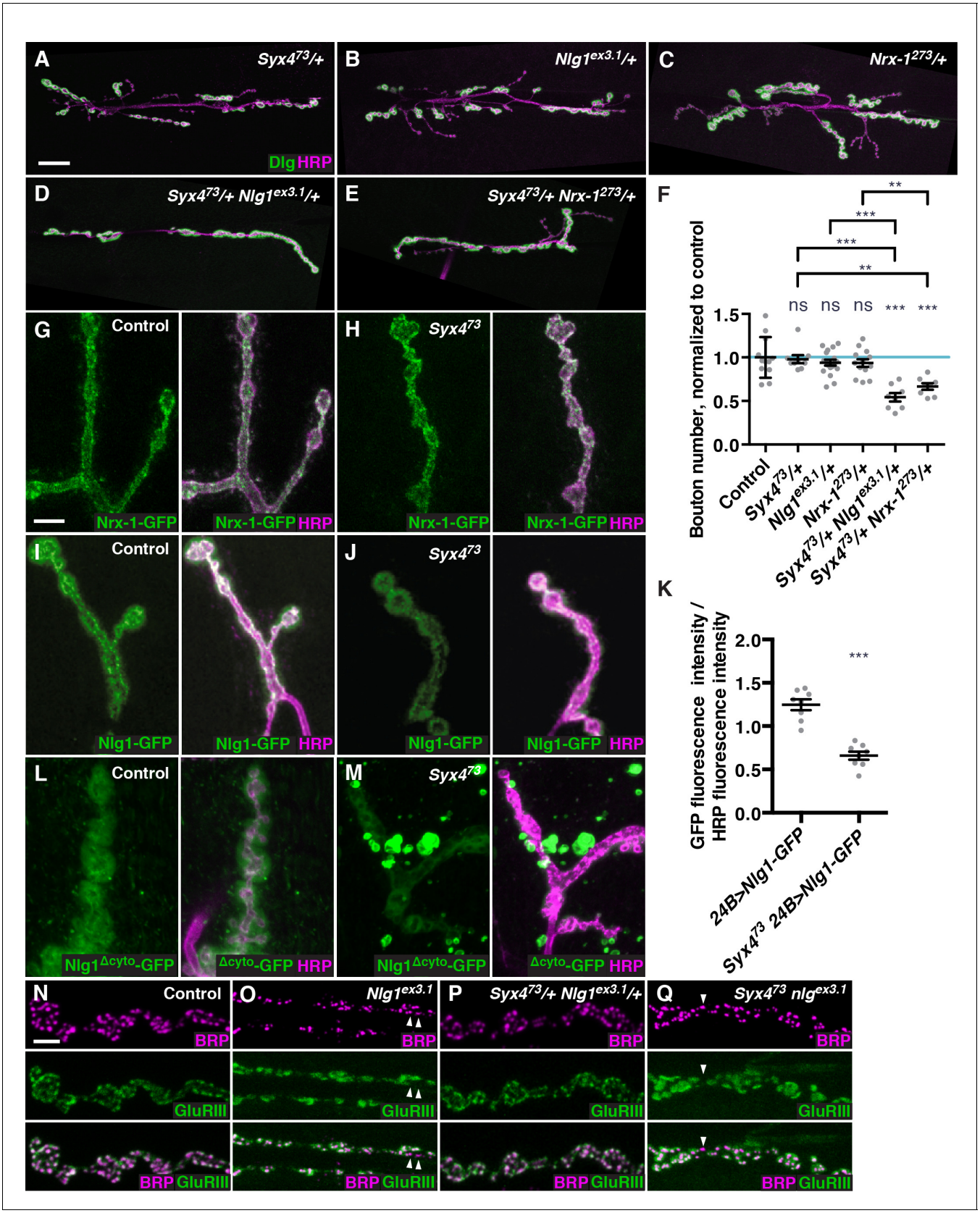

Figure 5. Syntaxin 4 interacts with Neuroligin 1 and regulates its membrane localization. (**A–E**), Representative images of NMJs stained with antibodies to the postsynaptic density marker Dlg (green) and the neuronal membrane marker HRP (magenta) to highlight the number of synaptic boutons;

Figure 5 continued on next page

Figure 5 continued

images are shown from *Syx4^{73}*/+ (**A**), *Nlg1$^{ex3.1}$*/+ (**B**), *Nrx-1^{273}*/+ (**C**), *Syx4^{73}*/+ *Nlg1$^{ex3.1}$*/+ (**D**), and *Syx4^{73}*/+ *Nrx-1^{273}*/+ (**E**) animals. (**F**) Quantification of bouton number, normalized to controls. Blue line indicates the control mean. Data are presented as mean ± SEM. (**G–H**), Representative images of NMJs stained with antibodies against HRP (magenta) and expressing Nrx-1-GFP in a control (**G**) or *Syx4^{73}* mutant (**H**) background. (**I–J**) Representative images of NMJs stained with antibodies against HRP (magenta) and expressing Nlg1-GFP in a control (**I**) or *Syx4^{73}* mutant (**J**) background. (**K**) Quantification of GFP fluorescence per HRP fluorescence from animals expressing Nlg1-GFP in a control or *Syx4^{73}* mutant background. Data are presented as mean ± SEM. (**L–M**) Representative images of NMJs stained with antibodies against HRP (magenta) and expressing Nlg1$^{\Delta cyto}$-GFP in a control (**L**) or *Syx4^{73}* mutant (**M**) background. (**N–Q**) Representative images of NMJs stained with antibodies against Brp (magenta) and GluRIII (green), from precise excision control (**N**), *Nlg1$^{ex3.1}$* (**O**), *Syx4^{73}*/+ *Nlg1$^{ex3.1}$*/+ (**P**), and *Syx4^{73} Nlg1$^{ex3.1}$* (**Q**) animals. Arrowheads indicate AZs lacking an apposed GluR field. Scale bars = 20 μm (**A–E**), 5 μm (**I,J,L–Q**). Statistical comparisons are fully described in ***Figure 5—source data 1***, and are indicated here as ***p<0.001, **p<0.01, *p<0.05, ns = not significant; comparisons are with control unless indicated.

DOI: 10.7554/eLife.13881.013

The following source data is available for figure 5:

Source data 1. Statistical data for ***Figure 5***.

DOI: 10.7554/eLife.13881.014

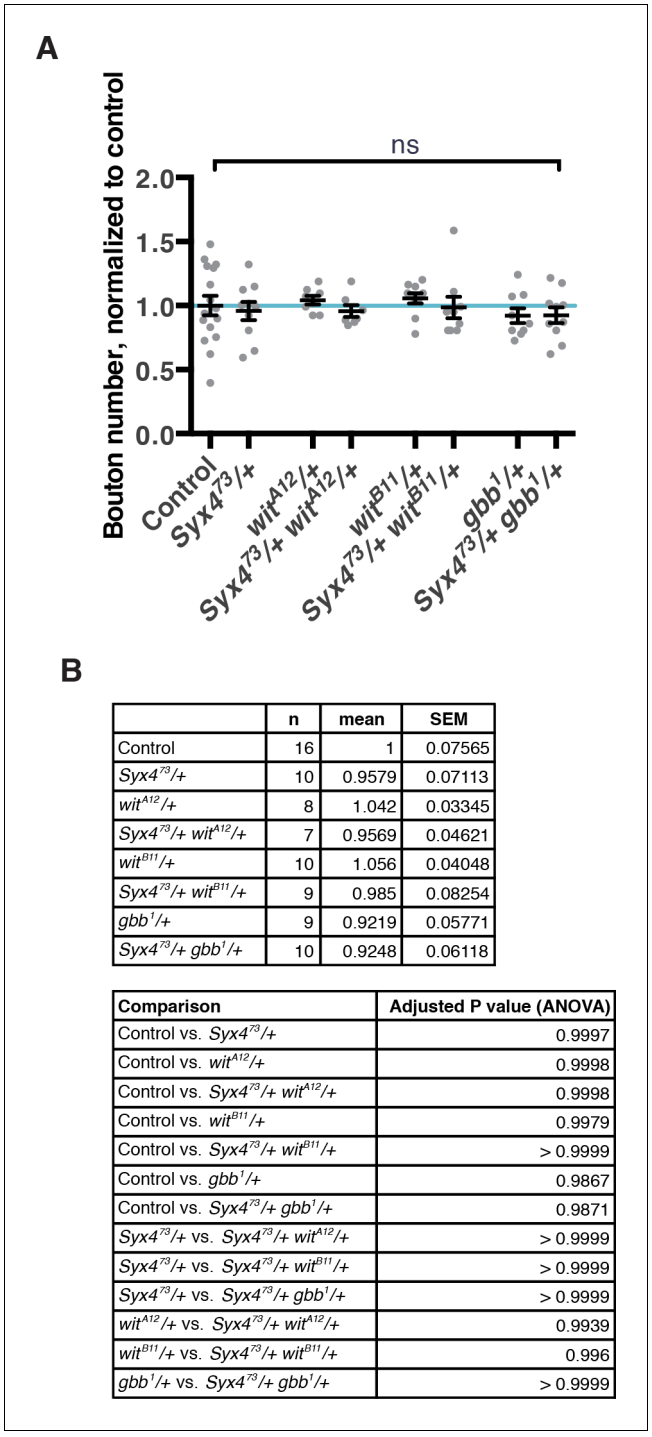

B

	n	mean	SEM
Control	16	1	0.07565
Syx4^{73}/+	10	0.9579	0.07113
wit^{A12}/+	8	1.042	0.03345
Syx4^{73}/+ wit^{A12}/+	7	0.9569	0.04621
wit^{B11}/+	10	1.056	0.04048
Syx4^{73}/+ wit^{B11}/+	9	0.985	0.08254
gbb^{1}/+	9	0.9219	0.05771
Syx4^{73}/+ gbb^{1}/+	10	0.9248	0.06118

Comparison	Adjusted P value (ANOVA)
Control vs. *Syx4^{73}/+*	0.9997
Control vs. *wit^{A12}/+*	0.9998
Control vs. *Syx4^{73}/+ wit^{A12}/+*	0.9998
Control vs. *wit^{B11}/+*	0.9979
Control vs. *Syx4^{73}/+ wit^{B11}/+*	> 0.9999
Control vs. *gbb^{1}/+*	0.9867
Control vs. *Syx4^{73}/+ gbb^{1}/+*	0.9871
Syx4^{73}/+ vs. *Syx4^{73}/+ wit^{A12}/+*	> 0.9999
Syx4^{73}/+ vs. *Syx4^{73}/+ wit^{B11}/+*	> 0.9999
Syx4^{73}/+ vs. *Syx4^{73}/+ gbb^{1}/+*	> 0.9999
wit^{A12}/+ vs. *Syx4^{73}/+ wit^{A12}/+*	0.9939
wit^{B11}/+ vs. *Syx4^{73}/+ wit^{B11}/+*	0.996
gbb^{1}/+ vs. *Syx4^{73}/+ gbb^{1}/+*	> 0.9999

Figure 5—figure supplement 1. Genetic interaction experiments between *Syx4* and BMP pathway components. (**A**) No genetic interactions are detected between *Syx4^{73}* and components of the BMP pathway: *wit^{A12}*, *wit^{B11}*, or *gbb^{1}*. Single and double heterozygous combinations are shown. Data are presented as mean ± SEM, ns = not significant. (**B**) Sample size (n), mean, SEM, and pairwise statistical comparisons are presented for the data in (A).
DOI: 10.7554/eLife.13881.015

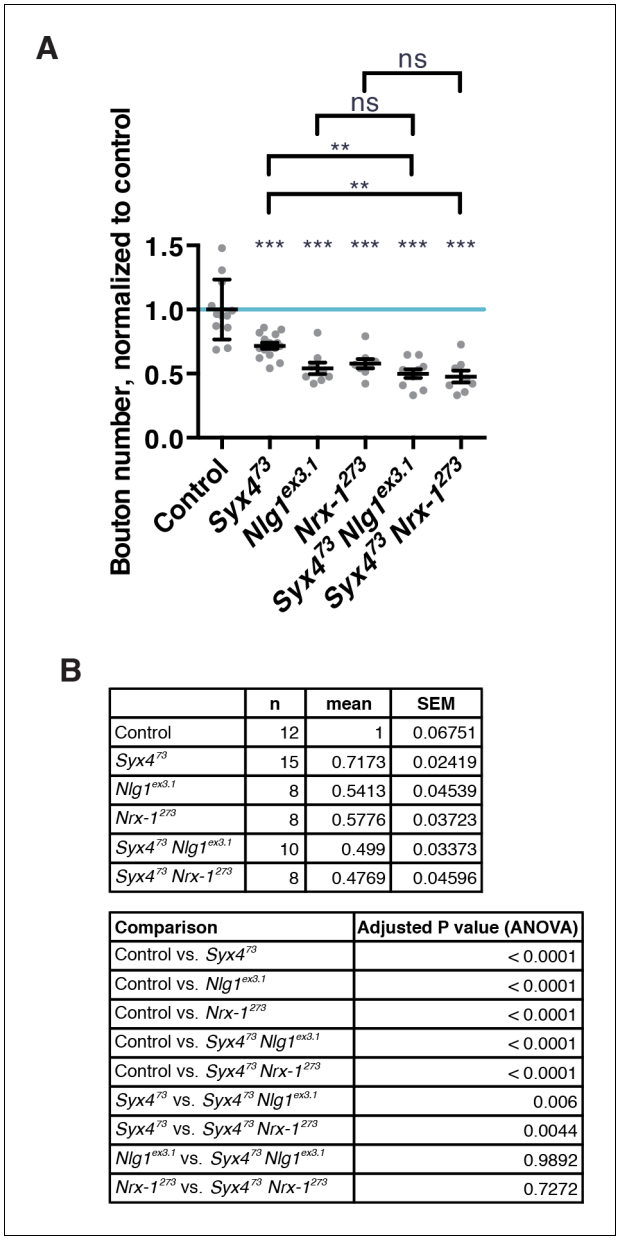

B

	n	mean	SEM
Control	12	1	0.06751
Syx4^{73}	15	0.7173	0.02419
Nlg1$^{ex3.1}$	8	0.5413	0.04539
Nrx-1^{273}	8	0.5776	0.03723
Syx4^{73} *Nlg1*$^{ex3.1}$	10	0.499	0.03373
Syx4^{73} *Nrx-1*^{273}	8	0.4769	0.04596

Comparison	Adjusted P value (ANOVA)
Control vs. *Syx4*^{73}	< 0.0001
Control vs. *Nlg1*$^{ex3.1}$	< 0.0001
Control vs. *Nrx-1*^{273}	< 0.0001
Control vs. *Syx4*^{73} *Nlg1*$^{ex3.1}$	< 0.0001
Control vs. *Syx4*^{73} *Nrx-1*^{273}	< 0.0001
Syx4^{73} vs. *Syx4*^{73} *Nlg1*$^{ex3.1}$	0.006
Syx4^{73} vs. *Syx4*^{73} *Nrx-1*^{273}	0.0044
Nlg1$^{ex3.1}$ vs. *Syx4*^{73} *Nlg1*$^{ex3.1}$	0.9892
Nrx-1^{273} vs. *Syx4*^{73} *Nrx-1*^{273}	0.7272

Figure 5—figure supplement 2. Genetic interaction experiments between single and double null mutants of *Syx4*, *Nlg1*, and *Nrx-1*. (**A**) Double mutants combinations between *Syx4*^{73}, *Nlg1*$^{ex3.1}$, and *Nrx-1*^{273} have severe synaptic growth defects. Data are presented as mean ± SEM. Statistical comparisons are indicated here as ***p<0.001, **p<0.01, *p<0.05, ns = not significant; comparisons are with control unless indicated. (**B**) Sample size (n), mean, SEM, and pairwise statistical comparisons are presented for the data in (A).
DOI: 10.7554/eLife.13881.016

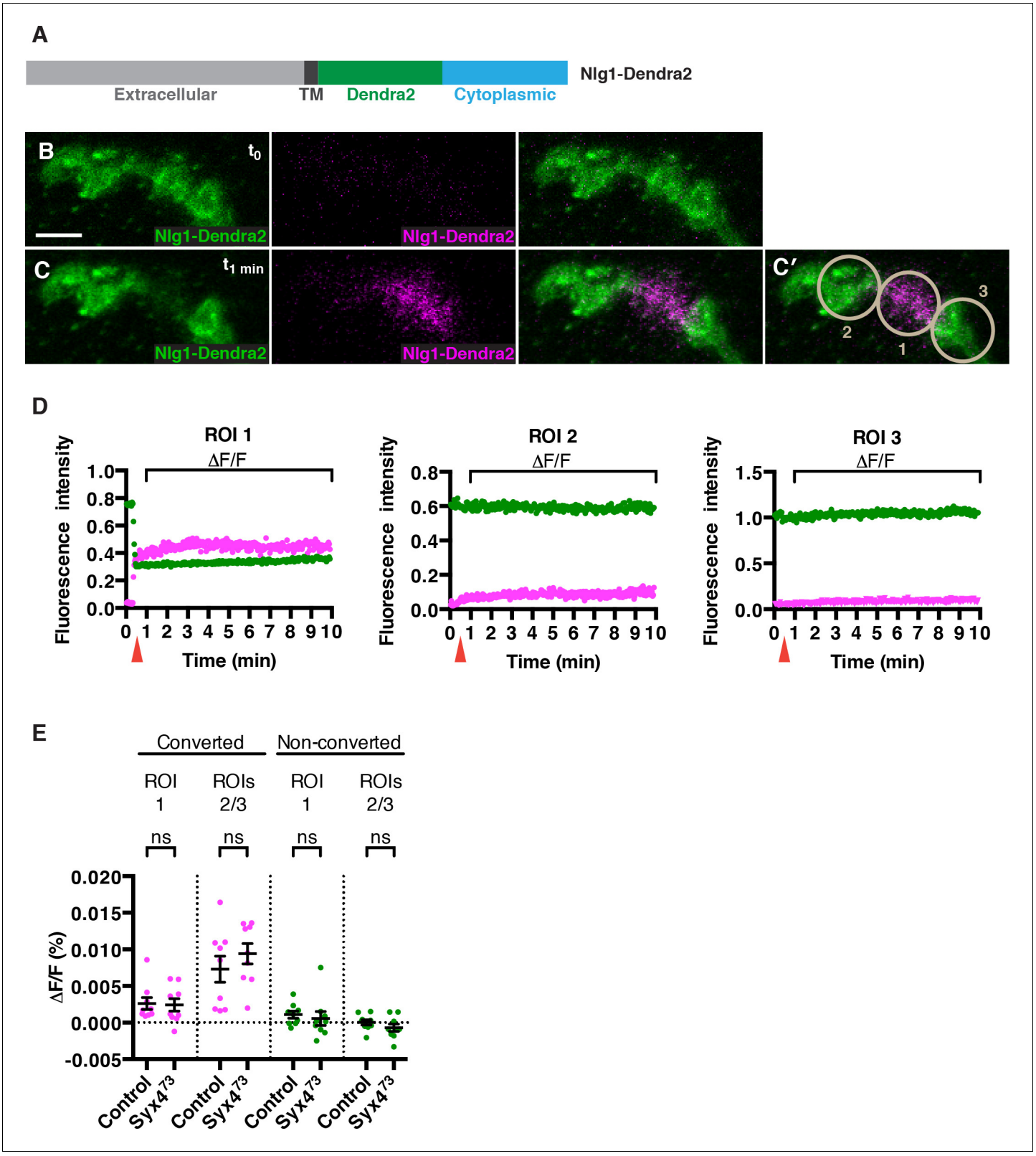

Figure 6. No change in mobility of Neuroligin 1 is observed in *Syntaxin 4* mutants. (**A**) Nlg1-Dendra2 construct. The Dendra2 tag was placed between the transmembrane domain and the cytoplasmic tail. (**B–C**) Representative image from a single animal expressing Nlg1-Dendra2 in the postsynaptic cell. One bouton (ROI1) was targeted with a 405 nm laser for photoconversion of the Dendra2 tag after 1 min. Non-photoconverted Nlg1-Dendra2 is shown in green and photoconverted Nlg1-Dendra2 is shown in magenta before (**B**) and immediately after (**C**) photoconversion. (**C′**) Regions of interest:

Figure 6 continued on next page

Figure 6 continued

ROI1, photoconverted region; ROIs 2 and 3, adjacent regions. (**D**) Fluorescent intensity over time for photoconverted and non-photoconverted molecules in all three ROIs. Red arrows indicate time of photoconversion. (**E**) Quantification of ΔF/F of both photoconverted and non-photoconverted molecules, in all three ROIs, in both the control and *Syx4*^{73} mutant backgrounds. Data are presented as mean ± SEM. Scale bars = 5 μm. Statistical comparisons are fully described in ***Figure 6—source data 1***; no significant differences found (ns = not significant).

DOI: 10.7554/eLife.13881.017

The following source data is available for figure 6:

Source data 1. Statistical data for ***Figure 6***.

DOI: 10.7554/eLife.13881.018

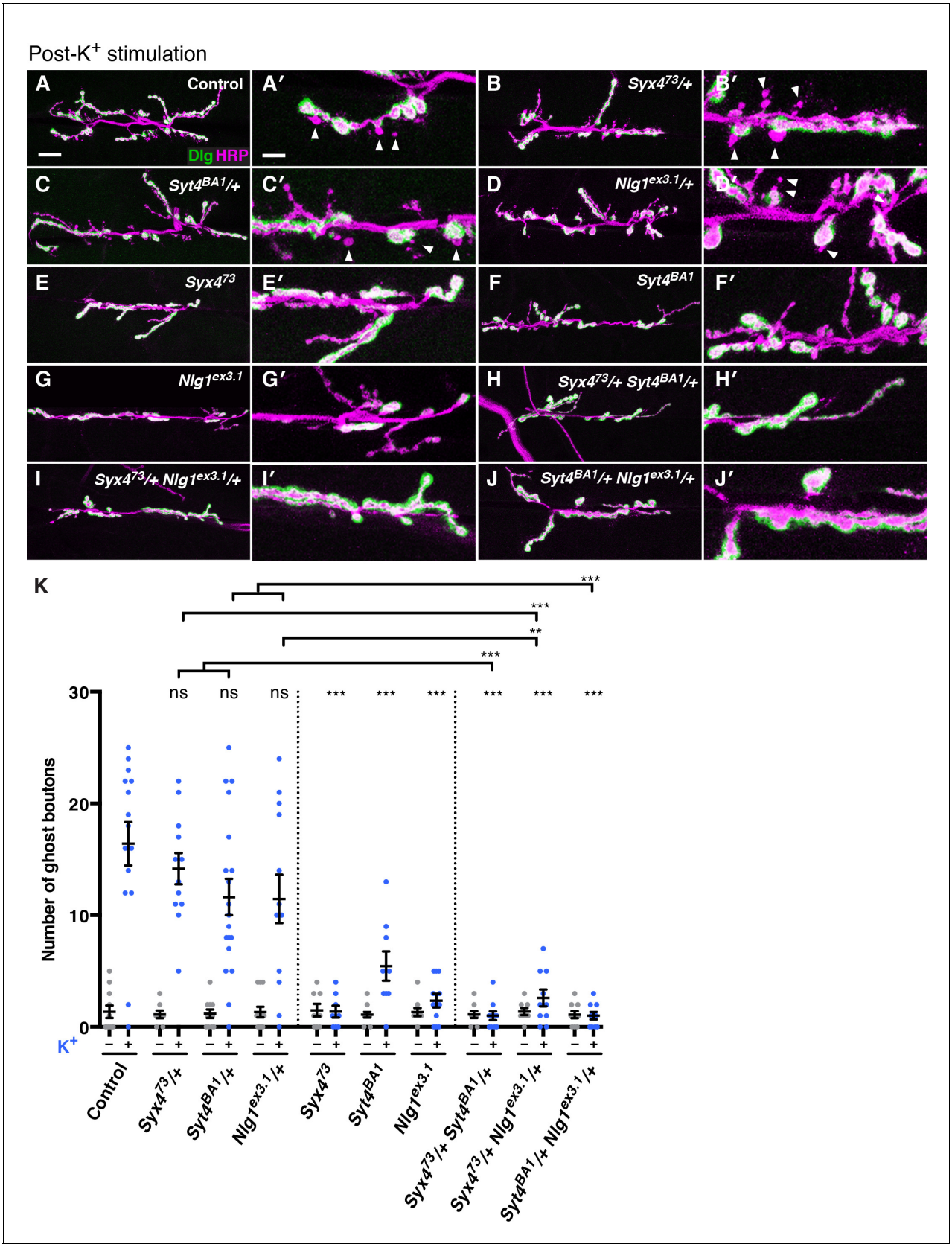

Figure 7. Syntaxin 4, Synaptotagmin 4, and Neuroligin 1 regulate acute structural plasticity at the NMJ. (**A–J**) Representative images of NMJs stained with antibodies to HRP (magenta) and the postsynaptic marker Dlg (green) to highlight synaptic boutons. Ghost bouton budding was stimulated with

Figure 7 continued on next page

Figure 7 continued

spaced incubations in high K^+. Ghost boutons are identified as round HRP+ structures lacking Dlg signal (arrowheads); images are shown from precise excision control (**A**), $Syx4^{73}$/+ (**B**), $Syt4^{BA1}$/+ (**C**), $Nlg1^{ex3.1}$/+ (**D**), $Syx4^{73}$ (**E**), $Syt4^{BA1}$ (**F**), $Nlg1^{ex3.1}$ (**G**), $Syx4^{73}$/+ $Syt4^{BA1}$/+ (**H**), $Syx4^{73}$/+ $Nlg1^{ex3.1}$/+ (**I**), and $Syt4^{BA1}$/+ $Nlg1^{ex3.1}$/+ (**J**) animals. (**K**) Quantification of ghost bouton number per NMJ from animals without (–) or with (+) high K^+ stimulation. Data are presented as mean ± SEM. Scale bars = 20 μm (**A–J**), 6.7 μm (**A'–J'**). Statistical comparisons are fully described in ***Figure 7—source data 1***, and are indicated here as ***p<0.001, **p<0.01, *p<0.05, ns = not significant; comparisons are with control unless indicated.

DOI: 10.7554/eLife.13881.021

The following source data is available for figure 7:

Source data 1. Statistical data for ***Figure 5***.

DOI: 10.7554/eLife.13881.022

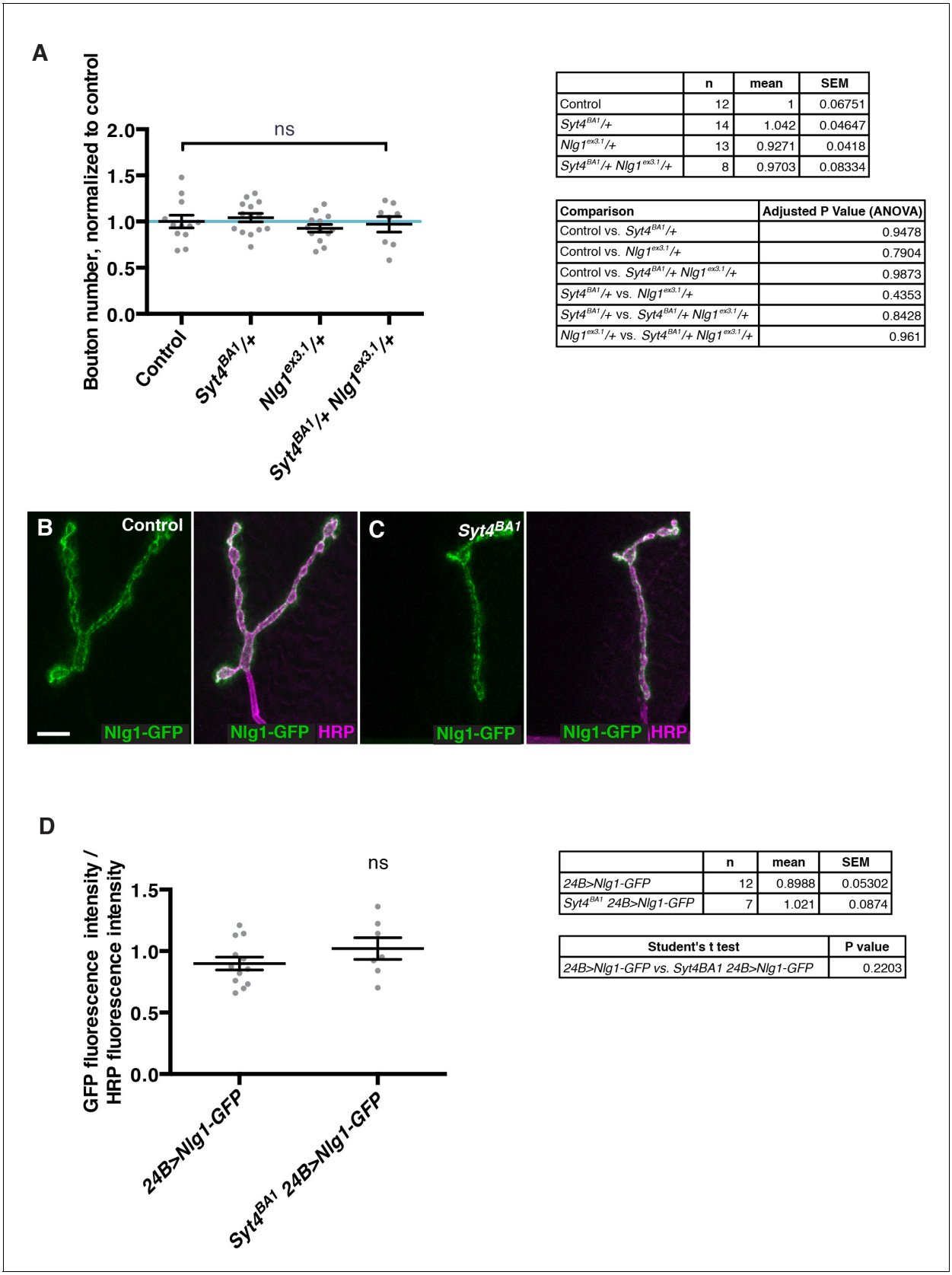

	n	mean	SEM
Control	12	1	0.06751
Syt4^{BA1}/+	14	1.042	0.04647
Nlg1$^{ex3.1}$/+	13	0.9271	0.0418
Syt4^{BA1}/+ Nlg1$^{ex3.1}$/+	8	0.9703	0.08334

Comparison	Adjusted P Value (ANOVA)
Control vs. *Syt4^{BA1}/+*	0.9478
Control vs. *Nlg1$^{ex3.1}$/+*	0.7904
Control vs. *Syt4^{BA1}/+ Nlg1$^{ex3.1}$/+*	0.9873
Syt4^{BA1}/+ vs. *Nlg1$^{ex3.1}$/+*	0.4353
Syt4^{BA1}/+ vs. *Syt4^{BA1}/+ Nlg1$^{ex3.1}$/+*	0.8428
Nlg1$^{ex3.1}$/+ vs. *Syt4^{BA1}/+ Nlg1$^{ex3.1}$/+*	0.961

	n	mean	SEM
24B>Nlg1-GFP	12	0.8988	0.05302
Syt4^{BA1} 24B>Nlg1-GFP	7	1.021	0.0874

Student's t test	P value
24B>Nlg1-GFP vs. Syt4BA1 24B>Nlg1-GFP	0.2203

Figure 7—figure supplement 1. Interaction experiments between Syt4 and Nlg1. (**A**) No genetic interactions are detected between *Syt4* and *Nlg1* with respect to bouton number. Data are presented as mean ± SEM, ns = not significant, ANOVA. Control refers to a precise excision control line for the

Figure 7—figure supplement 1 continued on next page

Figure 7—figure supplement 1 continued

Syt4^{BA1} allele. (**B–C**) Representative NMJs expressing Nlg1-GFP in control (**B**) or *Syt4*^{BA1} (**C**) backgrounds. (**D**) Quantification of GFP fluorescence intensity per HRP fluorescence intensity, in animals expressing Nlg1-GFP in control or *Syt4*^{BA1} backgrounds. Data are presented as mean ± SEM, ns = not significant, Student's *t* test. Scale bars = 5 μm. Sample size (n), mean, SEM, and pairwise statistical comparisons are presented for the data in (**A**) and (**D**).

DOI: 10.7554/eLife.13881.023